

Thermal Simulation and Analysis of the Single LED Module

*Dinh Van Quyen, Nguyen Nhu Nam, Nguyen Ngoc Anh, Nguyen Duc Tung,
Doan Quang Tri, Ta Quoc Tuan, Nguyen Duc Trung Kien,
Pham Thanh Huy, Dao Xuan Viet**

Hanoi University of Science and Technology, Hanoi, Vietnam

**Email: viet.daouxuan@hust.edu.vn*

Abstract

Light Emitting Diodes (LED) shows an important role in replacing traditional lamps due to their longevity, high efficiency, and environment-friendly operation. However, a large portion of the electricity applied on LED converts to heat, raising up the p-n junction working temperature, and lowering the output-light quality and the LED lifetime as well. Therefore, thermal management for LED is one of the key issues in LEDs lighting application. In order to investigate the impact of each component of the LED module on the junction temperature of the LED, we have performed thermal simulations of a typical single LED module by using the finite element method. Effects of thermal conductivity and thickness of each module's components on junction temperature were analyzed systematically. The results provided a detailed understanding of thermal behavior of a single LED module and established a crucial insight into thermal management design for high-power white LED lamp. Thermal-interface-materials (TIM) and the dielectric layer are proposed to have thermal conductivity around 1 W/mK for system optimization. In addition, based on the thermal analysis of heat sink, we have proposed and investigated a new configuration of plastic heat sink embedded with aluminum-alloy. The thickness ratio between the embedded aluminum layer and the heatsink base is suggested to be around 0.1 to 0.15 for the optimal configuration.

Keywords: LED, thermal management, finite element method

1. Introduction

High power light emitting diodes (LED) is one of the modern solid-state lighting devices which recruits semiconductor materials to generate light. LED lighting has more advantages than traditional light sources, i.g., high efficiency, long lifetime, fast response time, robustness and environmentally friendly. However, it converts a larger amount (75-85%) of input electric power into redundant heat [1, 2]. This heat ultimately increases the p-n junction temperature that causes many problems in optical performances as well as shortens the LED lifetime [3]. Therefore, thermal management is crucial in developing high power LED applications.

There are three parameters mainly impact the junction temperature: the input power, heat transfer performance of the system, and the ambient temperature. Typically, the input power and the ambient temperature are not controlled by thermal management for the LED-based luminaire. Rather, the heat transfer performance between the p-n junction and thermal reservoirs is needed to be optimized to minimize the junction temperature in use. There are two popular commercial LED modules nowadays: Chip-On-Board (COB) LED and Surface-Mount-Type

(SMT) LED. Recently, the thermal performance of all components of COB LED, including LED-chip, PCB, TIM, and heat sink, has been systematically studied using the finite element method (FEM) [1]. For instance, the PCB, commonly known as RF4 and MCPCB, have been studied about their heat conducting behavior [4,5]. The relationship between TIM's thermal conductivity and junction temperature has been investigated [6-9]. Heat sinks are also studied for their thermal behavior by the mean of FEM analyses (from the commercial FEA software). Besides, the thermal phenomena inside the SMT LED module have not been fully investigated. Thus, an overall picture of thermal phenomena of SMT LED module still remains in question.

In this study, we have symmetrically investigated the thermal performance of a single SMT LED module, including Osram Golden Dragon LED-chip, TIM1, PCB, TIM2, and heat sink by FEM/FEA software (shown in Fig. 2).

2. Modeling and Simulation

In this work, the single SMT LED module was modeled by utilizing the commercial software Abaqus 6.10. The schematic structure of the LED module

contains several components: LED, MCPCB, TIM and heatsink, as shown in Fig.1. LED is modeled based on the structure of the Osram Golden Dragon LED including p-n junction layer, metallization layer, die, die-attach and heat slug. The LED junction layer and metallization layer are very thin, potentially inducing numerous computational errors. Therefore, it is acceptable to remove those two thin layers in the FEM model. The MCPCB consists of three layers: a copper layer, a dielectric insulator layer, aluminum alloy layer. Next, the MCPCB connect to heatsink with the filling thermally interface material (TIM) into the gap between them.

Table 1. Dimension and properties of materials [1, 7]

Component	Materials	Thickness (mm)	Conductivity (W/mK)	
LED	LED chip	GaN	0.004	130
	Metallization	Au-Si bonding	0.01	27
	Die	Si	0.375	124
	Die-attach	Au-20Sn	0.05	57
	Heat slug	Cu	1.5	389
TIM	Grease	0.05	2	
PCB	Cu-layer	Cu	0.127	389
	Dielectric	Dielectric	0.075	1.1
	Al-alloy	Al-alloy	1	150
	Base			
Heat Sink	Al-alloy	-	166	

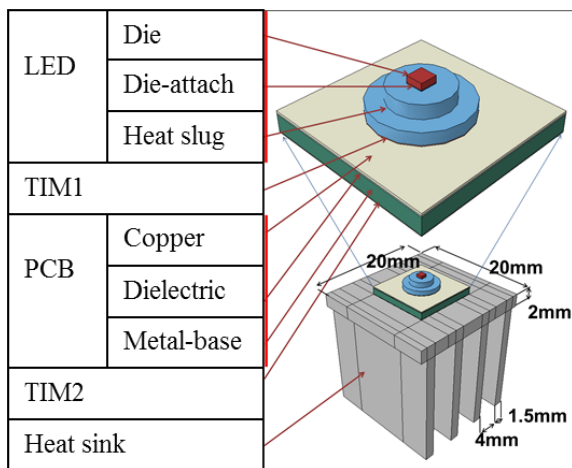


Fig. 1. Single LED module configuration.

We directly added the heat flux onto the Die component surface. As in the design, this silicon-Die is attached to the heat slug by a die-attach layer. The second main part is the printed circuit board (PCB) which includes three layers: the copper circuit layer, the dielectric layer, and the aluminum-alloy (Al-alloy) base layer. Third, with high thermal conductivity, the heat sink was attached to the module for the heat

dissipation purpose (Fig. 1) [10, 11]. These main parts were connected together by the layers of thermal interface material (TIM) which were also utilized to reduce the thermal resistance at the interfaces between the components. Details are shown in Table 1.

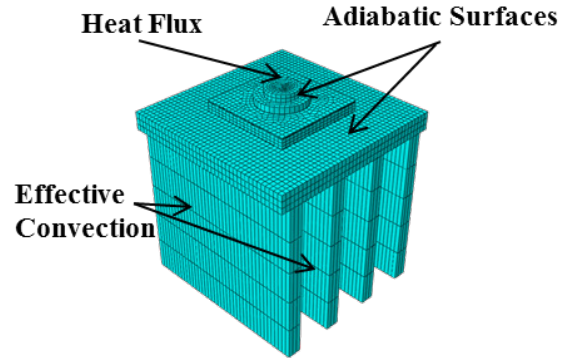


Fig. 2. FEA model of the single LED module.

The analytic element is assigned based on the input boundary conditions. From that, the equation of heat transfer, convection and thermal radiation in the model will be solved. At the LED junction layer, nearly eighty-five percents of the total electric power were converted into heat [12-14]. To study their inner heat dissipation phenomenon, we investigated the case of input power dissipated. The chosen heat source for the single LED module is 1W which is referred to various commercial Osram Golden Dragon LEDs data [1, 7].

The heat power was placed on the surface of the Die in the form of a heat flux since the heat flux from the junction layer technically flowed directly to the surface of the Die. For boundary conditions, the effective connectivity coefficient of 10 W/m²K [1], as previously mentioned, was applied to heat sink surfaces when the remains were set as adiabatic surfaces (Fig. 2) [15-17]. For meshing, linear hexagonal element shape was utilized for the whole model [1, 5, 8]. The number of elements in this single LED module model was set around 13500 for the most efficient computations. The thicker meshing still induced the unchanged results. The higher density of mesh is focused on the parts of heat sources interfaces such as Die and Die-attach.

The heat transfer used in simulations is governed by steady-state heat transfer Eq.(1) [18, 19].

$$k \left[\frac{\partial^2 T}{\partial x^2} + \frac{\partial^2 T}{\partial y^2} + \frac{\partial^2 T}{\partial z^2} \right] + Q - hA(T - T_{amb}) = 0 \quad (1)$$

where k is the thermal conductivity (W/mK), Q is the heat generation per unit volume (W/m³), h is the convective coefficient (W/m²K), A is the area (m²), T is the temperature (°C).

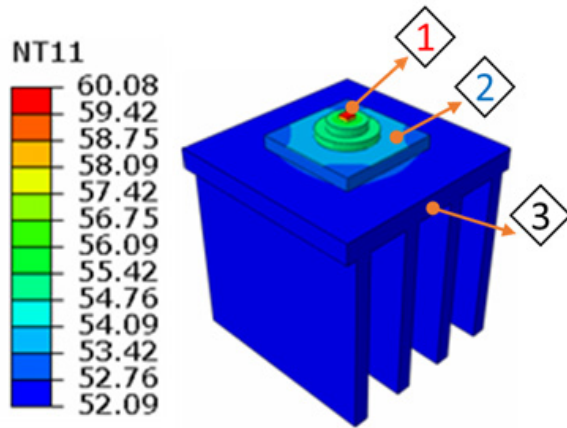


Fig. 3. Thermal distribution of single SMT LED module with of 25 °C ambient temperature

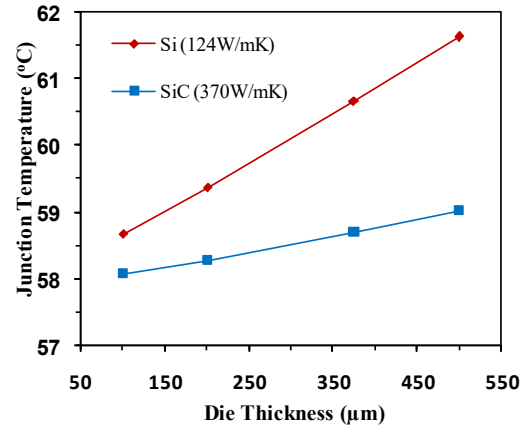


Fig. 5. Die thickness versus junction temperature

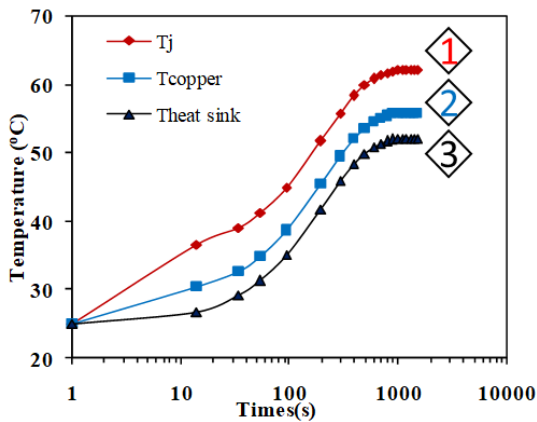


Fig. 4. The transient temperature of some of the main components of the LED module.

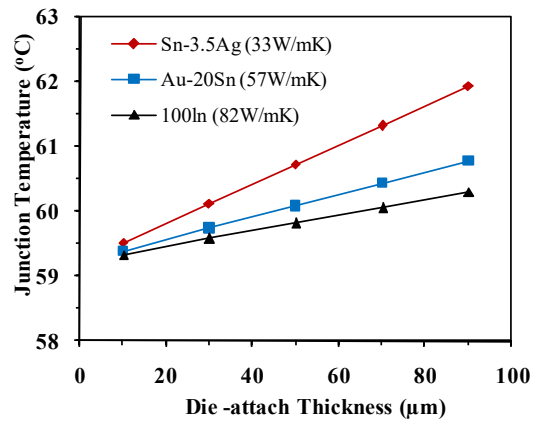


Fig. 6. Die-attach thickness versus junction temperature

3. Thermal Simulated Results

As mentioned above, because of the thin thickness of the p-n junction and the metallization, we assumed that the difference between p-n junction temperature and the Die temperature is very small.

To validate this assumption, simulations with and without these layers have been performed. The temperature difference between the two cases was only 0.3 °C. Therefore, the p-n junction and metallization layers were not modeled in our further simulations and analyses. In running simulation, we first evolved with the time-steady simulations.

Fig. 3 shows the temperature distribution of the single SMT LED module with simulated condition showing in Table I. The advantage of this time-steady simulation is the fast-outcome results with a small amount of calculation time. However, since the steady simulation cannot show the time-dependent temperatures of the system, we thus conducted transient simulations in order to fulfill the research purposes.

Fig. 4 demonstrates the transient temperature distribution of our single LED module containing the junction temperature (T_j), the temperature of the copper layer (T_{Copper}) and the average temperature of the heat sink ($T_{heat-sink}$). The result fully illustrates the behavior of any pointed local temperature of the system. The running time for temperature equilibrium is 800 seconds. In comparison, the results of the time-steady (Fig. 3) and the transient simulations show the consistency. Thus, we could use these both simulations for analyses.

The effects of LED module's properties on the junction temperature (T_j) have been systematically investigated with every single component: LED-chip, TIM1, PCB, TIM2, and Heat sink as following.

3.1. LED

Si and SiC materials are used for the Die of the LED-chip. By using FEA analysis, we have determined the relation between the change of the Die thickness and the T_j . The similar analyses have been also conducted for the Die-attach layer with the three utilized materials: Sn-3.5Ag, Au-20Sn, and 100In.

Fig. 5 and Fig. 6 present the tendencies that the increase of T_j is linearly dependent on the thickness growth of these layers. The role of material (thermal conductivity) grows when layer thickness increases. Thus, to avoid the must of use of a certain material, a wise choice should be made on thickness design. For example, a Die-attach in design, with a thickness smaller than 30 μm , is mostly independent of materials.

Heat slug is a metal block that conducts and spreads heat produced from the junction. The performance of a heat slug depends on its geometric structure and thermal conductivity. Thus, we show the comparison in using the five different materials for the heat slug as for cooling T_j , in Fig. 7. Among the basic materials used for heat slug, i.e., 46 W/mK of Al_2O_3 , 59 W/mK of Fe, 201 W/mK of Al and 380 W/mK of Cu, the copper heat slug facilitates the rapid heat dissipation and effectively reduces the Joule heating effect. As also shown in Fig. 7, the T_j drops rapidly

from approximately 67.5 $^\circ\text{C}$ to 61 $^\circ\text{C}$ when the heat slug's thermal conductivity ($k_{\text{heat-slug}}$) increases from 46 W/mK to 166 W/mK. Further increase of $k_{\text{heat-slug}}$ plays an insignificant effect on T_j which is only about 1 $^\circ\text{C}$. Thus, using a heat-slug with the thermal conductivity greater than or equal to 150 W/mK seems to be an appropriate design. The study has shown the familiar behavior with other researches [1, 19] in determining the relation between T_j and material properties of the LED-chip. However, we focus more on how to choose an effective material for each part of the LED-chip.

3.2. TIM1

The heat spreading process inside the module and the junction temperature are partly depended on the thermal conductivity and thickness of TIM layers.

Fig. 8 shows a special point that T_j reaches higher values dramatically when TIM1's thermal conductivity (k_{TIM1}) is smaller than 1 W/mK. However,

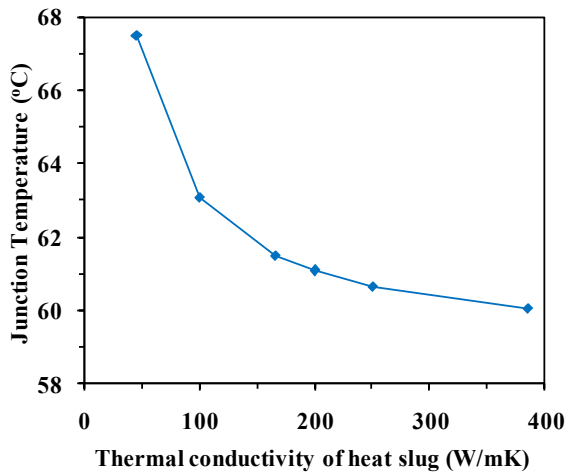


Fig. 7. Junction temperature as a function of thermal conductivity of heat slug of LED.

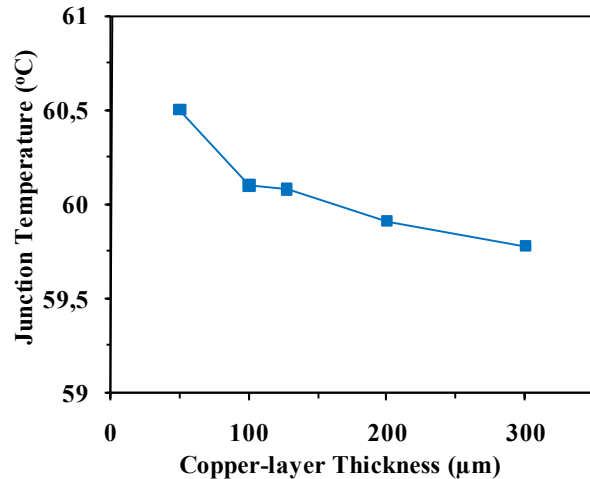


Fig. 9. The junction temperature is dependent on copper-layer thickness.

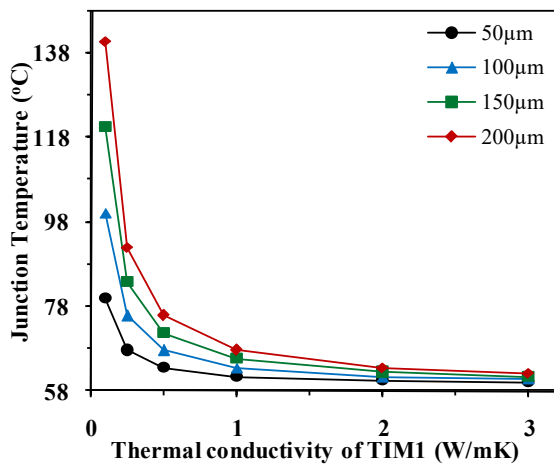


Fig. 8. Junction temperature versus thermal conductivities in various cases of TIM1 thickness.

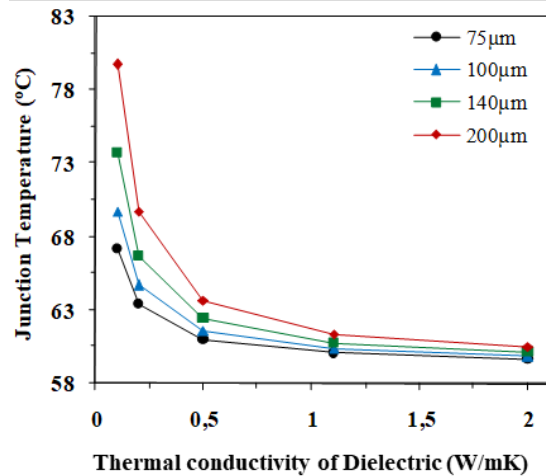


Fig. 10. Junction temperature as a function of thermal conductivities and thickness of the dielectric layer.

these results also present the weak dependence on the TIM1 thickness (d_{TIM1}) of T_j when k_{TIM1} gets higher than 1 W/mK. We thus suggest that the appropriate value of the thermal conductivity of TIM1 should be greater than 1 W/mK.

3.3. PCB

Fig. 9 to Fig. 10 show the weak contribution of the copper layer, dielectric layer and aluminum-base layers in cooling T_j . To be clear, the T_j gap between the minimum case (1 μm) and the maximum case (300 μm) of the copper layer's thickness (d_{Copper}) is only 1.2 $^{\circ}\text{C}$. Even though the copper layer has a constant thermal conductivity, the subsequent layers were still in full consideration of how their tested thermal conductivity and thickness cool down the T_j (Fig. 10 and 11). Fig. 10 illustrates the slight decrease of T_j undergoing the thickness reduction the dielectric layer ($d_{dielectric}$), except the $k_{dielectric}$ from 0.1 to 0.5 W/mK. When $k_{dielectric}$ is smaller than 1 W/mK, the T_j is in an accelerating increase. Thus, the optimal value of $k_{dielectric}$ for a suitably cool T_j is larger than 0.5 W/mK. Under the similar analysis for the dielectric layer, the thermal conduction ability of the Al-alloy base ($k_{Al-alloy}$) plays a poor effect on T_j .

In conclusion, when the PCB's analysis from other research [1, 5] was achieved for the type of COB module, our research has fully described how the T_j is affected by every individual portion of the PCB of the SMT module.

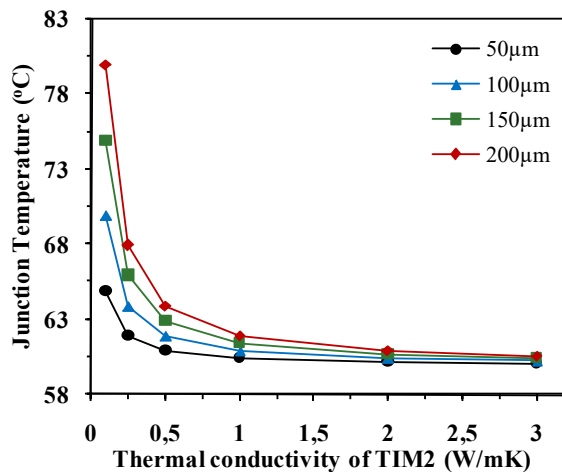


Fig. 11. Junction temperature as a function of thermal conductivities and thickness of TIM2.

Considering the five different thicknesses and the interval of 100 to 200 W/mK of thermal conductivity of the TIM2 layer, we can see how the TIM2 affects the T_j . As seen in Fig. 11, it is clear that T_j reaches high temperatures when k_{TIM} gets smaller than 0.5 W/mK. Compared with the case of the TIM1, the suitable materials for TIM2 could have a lower k_{TIM} , i.g, 0.5 W/mK for TIM2 and 1 W/mK for TIM1. The results can be useful for LED commercial applications.

3.4. Heat Sink

In heat sink analysis, Fig. 12 shows the dependence of the T_j on the thermal conductivity of the heat sink ($k_{heat-sink}$), which illustrates that the T_j is almost stable when $k_{heat-sink}$ is higher than 75 W/mK. However, the T_j will get higher when $k_{heat-sink}$ gradually decreases from 75 W/mK. Thus, the appearance of a heat-sink with a $k_{heat-sink}$ higher than 75 W/mK is necessary. On the other hand, the inserted graph in Fig. 12 presents the strong effect of the convective factor on cooling T_j . It is almost 100 $^{\circ}\text{C}$ of disproportion when the effective convective coefficient rises from 8 to 20 W/m 2 K. Thus, in the role of cooling off T_j , the plate-fin heat sink is proved its two important contributors: thermal conductivity and convective factor, that are directly related to the heat sink materials. Currently, plastic materials are commonly used to make various kinds of heat sink [20]. Therefore, besides the driver-potting material option [21], a study about the design of plastic heat sink embedded with aluminum component seems to be a potential solution for the thermal issue in LED lighting engineering.

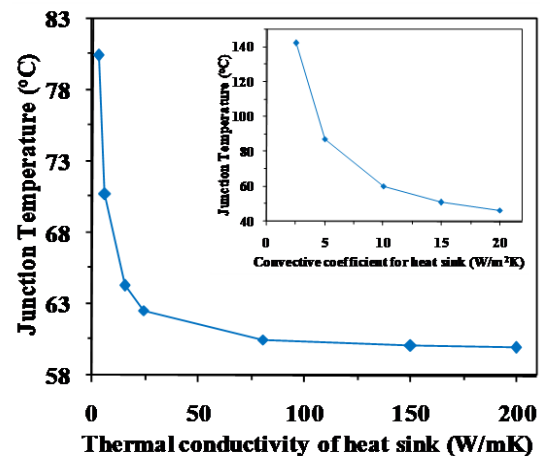


Fig. 12. Junction temperature as a function of thermal conductivities and convective coefficient (inset) of the heat sink

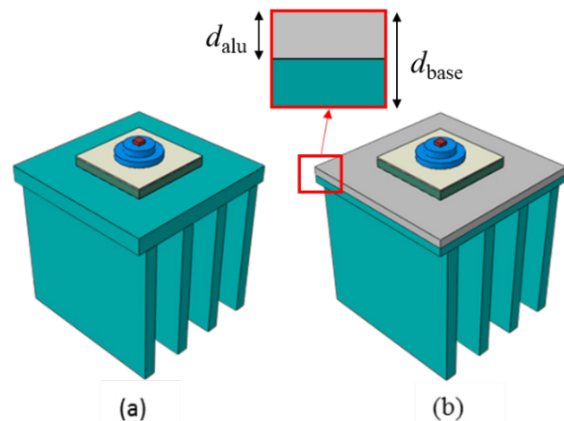


Fig. 13. Configuration of (a): plastic heat sink (TYPE1), (b): plastic heat sink embedding aluminum component (TYPE2)

4. Case Study: Plastic Heat Sink Embedded with Aluminum

The plastic heat sink (TYPE1) is potentially replacing the aluminum heat sink in commercial products because of its reasonable prices; however, its thermal conductivity is normally low (from 1 to 24W/mK) [20]. In order to balance the use of plastic and metal materials in producing an optimal heat sink, we study a model of plastic heat sink embedded with aluminum-component (called TYPE2) (Fig. 13).

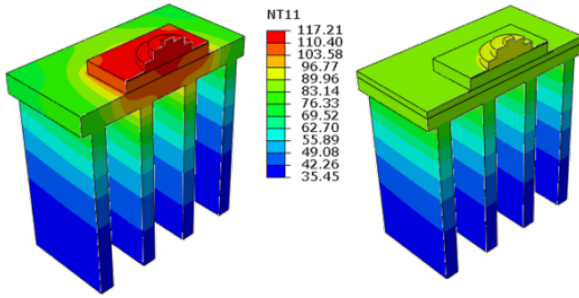


Fig. 14. Cross-sectional thermal distribution of TYPE1 and TYPE2 (with thin Al-alloy layer) respectively, at 1 W/mK of $k_{plastic}$.

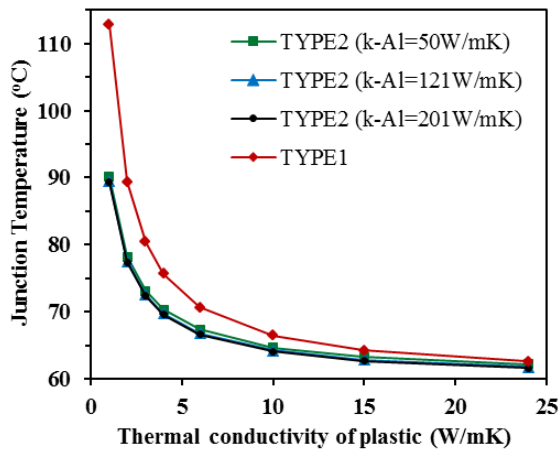


Fig. 15. Junction temperature depends on thermal conductivity of plastic in cases of the plastic heat sink (TYPE1) and the embedding heat sink (TYPE2)

Fig. 14 presents the dramatic down of T_j and the more uniform thermal distribution as a result when the plastic heat sink (TYPE1) embedding an aluminum component to become the TYPE2 heat sink. That is the interesting sign for deepening this case study.

Fig. 15 shows the relation between T_j and the $k_{heat-sink}$ of the two heat sinks. The curve with red color represents the T_j as a function of thermal conductivity of plastic ($k_{plastic}$) when using the plastic heat sink (TYPE1). The green, blue, and orange curves represent the change of T_j at the various cases of $k_{plastic}$ used in the TYPE2 with $k_{Al-alloy}$ is 50, 121, 201 W/mK, respectively. When the $k_{plastic}$ decreases, the T_j rises, however, the rapid increase of T_j occurs when $k_{plastic}$ is

smaller than 3W/mK. The largest T_j gap between the TYPE2 and TYPE1 is 23.5 °C at 1 W/mK of the $k_{plastic}$. This gap gradually decreases to 0.5 °C at 25 W/mK of $k_{plastic}$. Moreover, in the TYPE2, the use of different $k_{Al-alloy}$ in the range from 50 to 200 W/mK engenders no significant change in T_j . The use of one of the cheapest Al-alloy materials here ($k_{Al-alloy}=50W/mK$) for the design is enough.

Focusing on the thickness of aluminum-component in TYPE2, we calculus the new parameter x with:

$$x = d_{alu}/d_{base} \quad (2)$$

where x is the ratio of aluminum thickness in the heat sink base of the TYPE2 module, d_{alu} is the thickness of the aluminum-component, and d_{base} is the total base thickness.

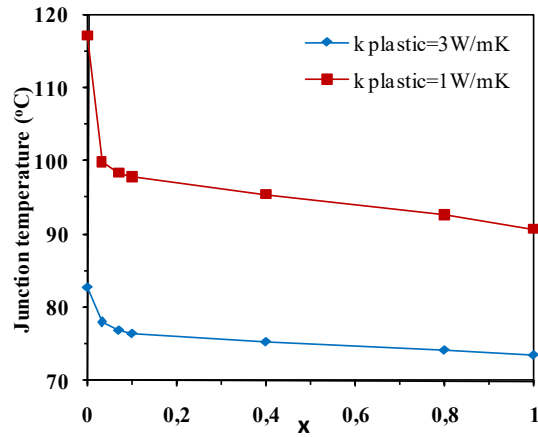


Fig. 16. Junction temperature versus thickness ratio of the aluminum- component in the TYPE2 module.

Fig. 16 demonstrates how T_j depends on x . T_j does not change much when x is in the range of 0.1 to 1, however, rockets to a high value when x turns to be smaller than 0.1. Therefore, even though the analysis shows the weak dependence of T_j on the d_{alu} when x is higher than 0.1, but once again proves the critical presence of the embedded aluminum in the TYPE2 model. To summarize, the results of this case study have indicated the weak dependence of T_j on k_{Al} and d_{alu} in all cases of TYPE2. However, for a particular point, T_j will be very high when $k_{plastic}$ less than 3 W/mK or the ratio x is smaller than 0.1. Therefore, the case study indicates that the TYPE2 is more advanced than TYPE1 in cooling T_j , especially in the use of a low $k_{plastic}$ model. And in case of using the TYPE2, it is better if an aluminum component could be embedded with a thickness just needed to be equal or larger than 0.1 d_{base} .

5. Conclusion

Both steady state and transient state simulations have been performed to investigate the junction temperature of our typical SMT LED module. The

simulation was used to analyze the thermal characteristics of each component in the module and how they contribute to the junction temperature. Effect of thermal conductivity and thickness LED module components on junction temperature were analyzed symmetrically. The main contribution of this work is to point out that the junction temperature strongly depends on the thermal conductivity of heat slug, TIM, and heat sink. Convective coefficient of heat sink plays an important role in heat dissipation of LED. Results this work can be used for effective thermal management design of the LED module.

In addition, the case study of the new configuration of the heat sink; aluminum embedded plastic heat sink has been investigated via thermal conductivity and geometric structure. The configurations are proved better than the pure plastic heat sink. The results give us a suggestion of the thermal design for use in the brand of low thermal conductivity plastic heat sink.

Acknowledgments

This work was supported by Hanoi University of Science and Technology under Project No. T2016-PC-015.

References

- [1]. M. Ha, S. Graham, Development of a thermal resistance model for chip-on-board packaging of high power LED arrays, *Microelectronics Reliability* 52 (2012) 836-844 and Ha's master thesis. <https://doi.org/10.1016/j.microrel.2012.02.005>
- [2]. M. Arik, C. Becker, S. Weaver, J. Petroski, Thermal management of LEDs: package to system, *Third International Conference on Solid State Lighting*, vol. 5187, 2004, pp. 64–75. <https://doi.org/10.1117/12.512731>
- [3]. J.J. Fan, K.C. Yung, M. Pecht, Lifetime estimation of high-power white LED using degradation-data-driven method, *IEEE Trans. Device Mater. Reliab.* 12 (Jun 2012) 470–477. <https://doi.org/10.1109/TDMR.2012.2190415>
- [4]. H. Dieker, C. Miesner, D. Puttjer, B. Bachl, Comparison of different LED modules, *Proc. SPIE 6797, Manufacturing LEDs for Lighting and Displays*, 67970I (2007). <https://doi.org/10.1117/12.758944>
- [5]. K. C. Yung, H. Liem, H. S. Choy, W. K. Lun, Thermal performance of high brightness LED array module on PCB, *International Communications in Heat and Mass Transfer*, 37 (2010) 1266-1272. <https://doi.org/10.1016/j.icheatmasstransfer.2010.07.023>
- [6]. K. Bai, L. G. Wu, Q. H. Nie, S. X. Dai, B. Y. Zhou, X. J. Ma, Z. Y. Zheng, Thermal study on high-power white LED down light, *Advanced Design Technology*, Pts 1-3, 308-310 (2011) 2531-2536. <https://doi.org/10.4028/www.scientific.net/AMR.308-310.2531>
- [7]. F. Hou, D. Yang, G. Zhang, Thermal analysis of LED lighting system with different fin heat sinks, *Journal of Semiconductors*, 32 (2011). <https://doi.org/10.1088/1674-4926/32/1/014006>
- [8]. Y. Yang, Numerical study of the heat sink with un-uniform fin width designs, *International Journal of Heat and Mass Transfer*, 52 (2009) 3473–3480. <https://doi.org/10.1016/j.ijheatmasstransfer.2009.02.042>
- [9]. J. V. Lawler, Thermal Simulations of Moduled IR LED Arrays, *SPIE 6942, Technologies for Synthetic Environments: Hardware-in-the-Loop Testing XIII*, 69420E (2008). <https://doi.org/10.1117/12.778719>
- [10]. A. L. Palisoc, C. C. Lee, Thermal-properties of the multilayer infinite-plate structure, *J. Appl. Phys.* 64 (1998) 410. <https://doi.org/10.1063/1.341442>
- [11]. K. Bai, L. Wu, B. Zhou, Thermal simulation and optimization of high-power white LED lamp, *Proc. IEEE, International Conference on Electronics, Communications and Control* (2011) 6067938. <https://doi.org/10.1109/ICECC.2011.6067938>
- [12]. Y. S. Muzychka, M. M. Yovanovich, J. R. Culham, Influence of geometry and edge cooling on thermal spreading resistance, *J. Thermophys. and Heat Transfer*, 20, 2 (2006) 247-255. <https://doi.org/10.2514/1.14807>
- [13]. Y. S. Muzychka, M. M. Yovanovich, J. R. Culham, Thermal spreading resistance in compound and orthotropic systems, *J. Thermophys. and Heat Transfer* 18, 1 (2004) 45-51. <https://doi.org/10.2514/1.1267>
- [14]. Y. S. Muzychka, J. R. Culham, M. M. Yovanovich, Thermal spreading resistance of eccentric heat sources on rectangular flux channels, *J. Electron Packag.* 125, 2 (2003) 178-185. <https://doi.org/10.1115/1.1568125>
- [15]. Y. S. Muzychka, M. Stevanovic, M. M. Yovanovich, Thermal spreading resistances in compound annular sectors, *J. Thermophys. and Heat Transfer* 15, 3 (2001) 354-359. <https://doi.org/10.2514/2.6615>
- [16]. P. Kulha, J. Jakovenko, J. Formanek, FEM thermal mechanical simulation of low power LED lamp for energy efficient light sources, *Proc. ICREPQ'12, Spain* (2012). <https://doi.org/10.24084/repqj10.815>
- [17]. L. Huang, E. Chen, D. Lee, Thermal analysis of plastic heat sink for high power LED lamp, *Proc. IEEE, CFP1259B-ART*, (2012) 197-200. <https://doi.org/10.1109/IMPACT.2012.6420272>
- [18]. G. Velmathi, N. Ramshanker, S. Mohan, Design, electro-thermal simulation and geometrical optimization of double spiral shaped microheater on a suspended membrane for gas sensing, *Iecon 2010 - 36th Annual Conference on IEEE Industrial Electronics Society*, 2010. <https://doi.org/10.1109/IECON.2010.5675550>

- [19]. J.N. Reddy, *An Introduction to the Finite Element Method*, vol. 2, McGraw-Hill, New York, 1993.
- [20]. D. Christen, M. Stojadinovic, J. Biela, Energy efficient heat sink design: natural versus forced convection cooling, *IEEE Trans. Power Electron.* 32 (Nov 2017) 8693–8704.
<https://doi.org/10.1109/TPEL.2016.2640454>
- [21]. N. Nguyen, V.Q. Dinh, T. Nguyen-Duc, Q.T. Ta, X.V. Dao, T.H. Pham, T.K. Nguyen-Duc. Effect of potting materials on LED bulb's driver temperature. *Microelectronics Reliability.* 2018 Jul 31;86:77-81.
<https://doi.org/10.1016/j.microrel.2018.05.012>